MatLab Simulation of Self-Consumption in Small Photovoltaic Panel Energy Application: A Case Study in Estonia

Andres Annuk*‡, Wahiba Yaïci **, Vasilij Sudachenko ***, Toivo Kabanen*, Peep Miidla ****

* Chair of Energy Application Engineering, Institute of Technology, Estonian University of Life Sciences, 51006 Tartu, Estonia

** CanmetENERGY Research Centre, Natural Resources Canada, 1 Haanel Drive, Ottawa (Ontario), K1A 1M1 Canada

*** Institute for Engineering and Environmental Problems in Agricultural Production (IEEP) – branch of FSAC VIM, 73912808 Saint Petersburg, Russia

**** Estonian Centre of Industrial Mathematics, EE51009 Tartu, Estonia

(andres.annuk@emu.ee, wahiba.yaici@canada.ca, vnsud.alla@gmail.com, peep.miidla@gmail.com)

‡Corresponding Author; Andres Annuk, Estonian University of Life Sciences, 51006 Tartu, Estonia, Tel: +372 55682624 andres.annuk@emu.ee

Received: 12.08.2021 Accepted:29.09.2021

Abstract- Modern residential buildings are only sometimes equipped with independent energy sources such as wind generators, PV panels or similar sources from which green energy is generated. Experts predict that prosumers who concurrently produce and consume electricity will soon emerge en masse. Due to fluctuating and intermittent renewable energy sources, this dual process can increase the burden on the electricity grid. In this article, a process simulation of the energy supply of a residential building is developed, with PV panels as the independent source of electricity. The studied parameters of the prosumer nanogrid are a non-shiftable electrical load graph and a separate load graph of warm water consumption with a battery that ensures energy needs from the non-shifting load graph. For the annual simulation, we use measurement data with an average interval of 5 minutes. The article models and simulates energy flow graphs that will depend on consumption and production schedules and the size and design of storage devices, such as a buffer battery between the nano- and utility grid. If we double PV production compared total consumption and buffer battery 10 kWh as the same, we get the whole cover factor for the resultant increase Δ = 0.139. It means that the increment is 23 % in relative units. The novelty of the work is using a buffer battery between nano- and utility grids to increase the own consumption of PV electricity. One of the article's outputs compares the same nanogrid configuration with the wind generator instead of the PV panels as a local energy source. The results show that PV panels require significantly lower battery and water heater volumes than a wind generator to achieve the same demand cover factor. Compared to the power generation of PV panels with the wind generator, the inverter's power can be reduced to half the capacity without significantly reducing the demand cover factor.

Keywords Load shifting; energy storage; solar energy; self-consumption; cover factor; nanogrid; battery storage; distributed generation.

Nomenclature

LMI – Load Matching Index
LGMI – Load Generation Matching Index
PV – PV panels
NG – nanogrid
UG – utility grid
BB – buffer battery
SB – nanogrid storage battery
BO – hot water consumption in kWh
Y_D – the demand cover factor
W_1 – the sum of the annual production of PV, which is at first hand consumed by NS needs
W_2 – the sum of the annual production of PV, which is used for BO from WH

W_3 – the sum of the annual production of PV used for the NS consumption pattern from the battery annually
W_4 – the energy that moves back from BB to NG. If there is not enough energy for consumption needs in SB and WH, it will be taken from BB
W_{total} – the energy consumed in patterns NS and BO or otherwise, all energy consumed for the needs of a private house
Q – variable, depending on current situations
Q_{PV} – the 5-min energy production from PV
Q_{NS} – the 5-min energy consumption of graph NS
Q_{WH} – the 5-min energy feed-in WH
Q_{BO} – the 5-min energy consumption of BO graph
C_{WHmax} – as set the maximum capacity of WH in the particular calculation step
C_{WH} – the current energy content in WH, but not more than C_{WHmax}
C_{SBmax} – as set the maximum capacity of SB in the particular calculation step
C_{SB} – the current energy content in SB, but not more than C_{SBmax}
C_{BBmax} – as set the maximum capacity of BB in the particular calculation step
C_{BB} – the existing energy content of BB, but not more than C_{BBmax}
R_S – the amplification coefficient, the ratio of annual PV or wind production to the yearly consumption
P_{nom} – rated power of PV or wind generator

1. Introduction

The European Union's energy policy envisages the attainment of 32% renewable electricity from the total electricity generation portfolio by 2030 [1]. Achieving this commendable target requires increasing the share of wind and solar energy (available almost anywhere) in the renewable energy portfolio [2].

Simultaneously, wind and solar energy conversion do not have an exhaust thermal energy component for energy conversion [3]. Increasing self-consumption in microgrids is essential for reducing grid losses and securing 'rotating reserves' in the transmission network [4, 5]. Some microgrids can also employ super-capacitors [6] with batteries to allow for higher power energy exchanges with batteries than possible with battery-based storage. At the same time, a typical microgrid will probably have power exchanges with storage devices in the order of magnitude that the batteries can handle. Therefore, there would be no requirement for super-capacitors. Ravada et al. [6] and Kotra et al. [7] are looking at the storage device's capacity as a single unit, considering only the extent of its storage element.

A multi-period optimal power flow problem occurs and involves scheduling the charging/discharging of the electrical energy storage system over an extended planning horizon, e.g., for day-ahead operational planning is used to optimise a distribution system with energy storage systems [8]. Kusakana [9] optimises the cooperation of prosumers of PV power connected to the grid to reduce the cost of electricity and reduce the payback time of the prosumers. Self-consumption increases are considered at the level of poly-generation systems [10]; one element is also PV panel production. An optimal configuration of various production equipment will increase the cover factor. Excess solar energy in summer could be used for cooling [11]. Still, in the Baltic region, which is located in temperate zones, where the need for summer cooling is low and is becoming smaller due to global warming, the need for it is modest. The load-shifting approach is introduced to enable stochastic energy sources such as solar and wind output to be used to cover consumption schedules as much as possible [12-15]. Baetens [16] defined self-consumption and called it the “cover factor”. However, some scientists offer different explanations of cover factors, such as the Load Matching Index (LMI) or Load Generation Matching Index (LGMI) [17, 18]. Previous works [19, 20] have used storage equipment such as a water tank and battery to increase the cover factor in the nanogrid, and the energy is powered by wind and sun. Other studies referenced earlier took advantage of the balancing effect between the annual production schedules for wind and solar energy. The energy ratio was 70/30 %, with wind energy having a higher proportion of wind. One of the distinctive simulation studies [21] is carried out to increase local consumption by using a wind generator as a renewable energy source based on weather forecasts. However, the study did not use a functioning weather forecast but instead carried out the simulation based on a wind generator production data set. The supply cover factor increased by 8.8 %. If this method is employed for local PV generation, the outcome may be better since a more certain periodicity is observed when solar energy is received.

Connecting microgrids to an electric network through a battery has been covered quite a lot in scientific literature. Still, there are no articles in recent publications about increasing own consumption this way. For example, according to the source [22], the battery connected between the microgrid and the power grid reduces the character of intermittence of PV’s power, which infects the electrical grid's stability. Sometimes used battery between the microgrid and utility grid to decrease the daily operational and trading cost of the charging station [23] or improve energy quality [24]

Since the production of PV panels (PV) is DC, microgrids are also developed, which are either partially or wholly based on the DC bus [25-27].

The present study aims to simulate and configure buffer battery (BB) configuration between nanogrid (NG) with PV generation and utility grid (UG) to augment self-consumption. The principal outcome of the work lies in finding the system’s parameters and compare with the analogous nanogrid powered by the wind generator. In [28], peak load shaving is modelled mathematically through load-shifting energy on the demand side and settled using the optimisation model. Energy storage of the big-scale PV panels applications is handled on [29].

The work’s novelty is using a buffer battery between NG and UG to increase NG’s own consumption. However,

the impact of the ratio between production and consumption on self-consumption has also been examined. In addition, two similar wind and PV-powered systems have been compared.

2. Simulation Analysis

The model used (Figure 1) in the simulation study is based on a classic private residence electrical installation with an additional BB between the local NG and UG. The word microgrid, in this case, more specifically nanogrid, means an electrical installation powered by a local source of electricity with an energy storage and electricity network connection [30].

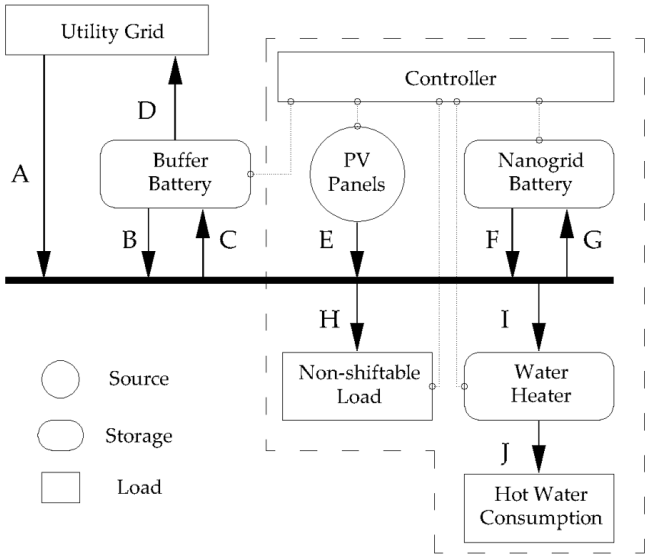

Figure 1. Energy currents between nanogrid (NG) and utility grid (UG): NG with (BB)

Figure 1 depicts the case study solution structure. Arrow A shows the direction of (costly) energy taken from the UG to cover energy shortages. The NG has an external BB electricity storage unit. Arrow B denotes power released to the NG – previously stored on BB (Arrow C) for free for the homeowner, produced by a PV, and surplus from residence consumption. Arrow D presents the possibility that the PV size is selected correctly, and part of the energy goes to UG.

In the simulation study, we first assessed the principles of managing energy currents in a private house (powered by PV) and exported them to the utility grid. The load controller (see Figure 1), "Controller", regulates the routing of energy powered by the PV. The bidirectional energy flows between the load controller and BB or UG are the energy flows between the load controller and nanogrid storage battery (SB). Single-acting energy flows are from PV to load controller, load controller to NS and WH. The SB battery (Figure 1, Arrows F and G) is designed to supply the NS consumer with energy shortage.

In contrast, the battery is supplied primarily with remnant NS consumption in a surplus of energy. BB battery is located between NG and UG (Figure 1, A, Arrows B and C) and will take the energy leftover from NG to get it back there on the first chance; if BB does not have enough power to supply NS, it will be taken directly from the network. If BB is complete and the energy flow from the NS direction continues, redirect it to UG.

The 2.5 kW PV station data was measured on the roof of the Institute of Technology of Estonian University of Life Sciences, in the Tartu city area (N 58.388458, E 26.694000) 01.12.2015-30.11.2016. The dataset collected covers the period from the 1st of December 2015 to the 30th of November 2016. PV production and consumption data were measured in the logger with a fixed 10 s, actually fluent between 2 and 24 s. Then, using cube interpolation, the data was converted to a form where the time series was formed from power data in the range of 10 s. Then we find a 5-minute average based on the values of the 10-second measurement periods within this time span. In this way, a time series of arithmetic mean powers of 5-min was formed. After these conversions, the power of the 5-min ranges was divided by 12, and the energy content of the 5-min ranges we use in the calculations was obtained.

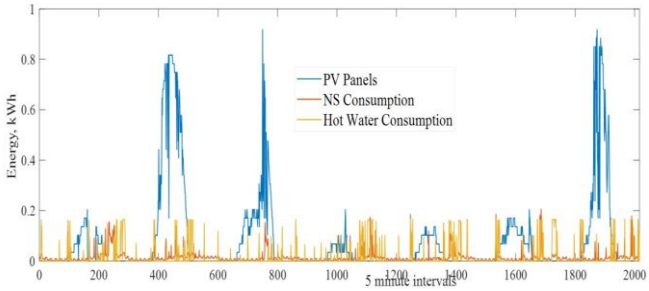

Figure 2. Sample data for the week of 1st–8th March 2016.

Subsequently, we scaled the annual energy output of PV to equal consumption while the nominal capacity of PV also changed. The rated power of PV increases to 3.67 kW. The following literature sources have studied the receipt and use of time series at 5-min average intervals [31-34].

The capacity of the batteries used in this study is not their nominal capacity. The capacity used in work can be defined as the capacity between the maximum battery capacity and the minimum permissible charge. The efficiency, power losses and ageing-related reduced capacity are not considered. WH, by analogy with the battery, only WH's active heat capacity is used. This is the thermal capacity of the water in the WH, which lies between the minimum and maximum permissible water temperatures.

Figure 2 depicts the production of one-week PV in 2016, and NS and hot water consumption (BO) consumption charts on the x-axis shows 2016 pieces of the 5 min average time interval (one week). The y-axis shows the average capacities of these ranges' production and consumption graphs. Figure 2 shows that the energy flow from PV is less frequent but more powerful, while those consumed are more frequent and weaker.

The annual output of the PV is scaled to match precisely the yearly load. In this respect, it should be noted that the level of solar radiation varies from season to season in Estonia. In the winter months, the production of PV parks is in Estonia. In the winter months, the output of PV parks is almost non-existent; in summer, on the contrary, solar energy is overabundant. A classical private residence load graph is considered NS and BO parts. The saved annual electricity consumption was 3473 kWh, with 47% (1632 kWh) being allocated to NS, and 53% (11841 kWh) to BO, based on actual, registered data [35]. The nanogrid configuration principle is described in [36], but PV is currently used as the renewable energy source interval.

The given model is drawn up based on the principles set out in the sources [16, 37] and belongs to multi-period multiple time scales over the year type [38]. Thus, the simulation results reflect the results for one particular year.

If consumers (NS and BO) do not need energy during the current period and it does not fit in the storage equipment, it will move on to BB and, if there is no space there, to UG. Further, the cover factor is evaluated for different scenarios. In literature, formulas of the cover factor are presented in different ways. We use the following equation (1) [39]:

$$Y_D = (W_1 + W_2 + W_3 + W4)/W_{total} \quad (1)$$

where:

Y_D is the demand cover factor;

W_1 is the sum of the annual production of PV, which is at first hand consumed by NS needs;

W_2 is the sum of the annual production of PV, which is used for BO from WH;

W_3 is the sum of the annual PV production used from the battery's NS consumption pattern annually. This is the case where PV cannot directly power the NS, and then the missing energy is taken from the batteries if there is one;

W_4 is the energy that moves back from BB to NG. If there is insufficient energy for consumption needs in SB and WH, it will be taken from BB. The use of this method for nanogrid powered by PV panels is novel. This energy flow is depicted with Arrow B in Figure 1 and is crucial to finding a new cover factor, Y_D. If there is not enough power in the BB, the missing part of the energy is taken directly from the UG, as shown by Arrow A in Figure 1;

W_{total} is the energy consumed in patterns NS and BO or otherwise, all energy consumed for the needs of a private house.

When the energy from the PV in the 5-min run has been compared to the NS requirements, the controller will decide on the NS's energy needs a source.

If the PV does not receive enough energy for NS, the missing energy is taken from SB.

If inequality $Q_{PV} > Q_{NS}$ is true, then the surplus energy to meet NS needs will move to SB if SB is full to WH.

Suppose WH is full; then energy moves to BB. In case of lack of additional space for energy in BB, then to UG.

If inequality $Q_{PV} > Q_{NS}$ is not valid, it will be taken short of energy from SB; if it is not enough, it will be taken from BB or, in case of a lack of energy in BB, from UG.

Figure 3 has been simplified for better insight. After filling the WH from the PV through the NS, the scheduled energy BO consumption is taken from the WH. If there is more space in the WH, additional PV energy will be added through the NS. This part of the program is not shown in Figure 3.

The block "Export excess energy to BB" is denoted in Figure 1 as Arrow C.

The peaks of the PV generation schedules correspond to the relatively small amount of energy, which could allow for a noticeably reduced power rating of the inverter without a significant impact on the cover factor. This can potentially enable specific cost savings.

The decision-making blocks formally concern a single sequence process, which starts with the assessment that the energy produced by the PV at the i-th of the 5-minute interval can be fully supplied to the NS consumer. The following order of transmission and allocation of energy is as follows: WH, BB and UG. If not PV produces enough energy for NS consumption, it is taken from SB or followed by BB or UG. If the energy generated by PV is leftover from NS consumption, then priority will be given to adding the surplus to SB first. Such a sequential process [39] is technically possible, where the Smart Meter distributes energy flows as follows: first, to UG, the remaining energy to the NS (here is also included in NS with BO), and finally, using a particular additional module, all the remaining energy, as far as it is received, goes to BO.

Figure 3 illustrates the flowchart of the developed nanogrid algorithm based on the operating principle of the system configuration shown in Figure 1.

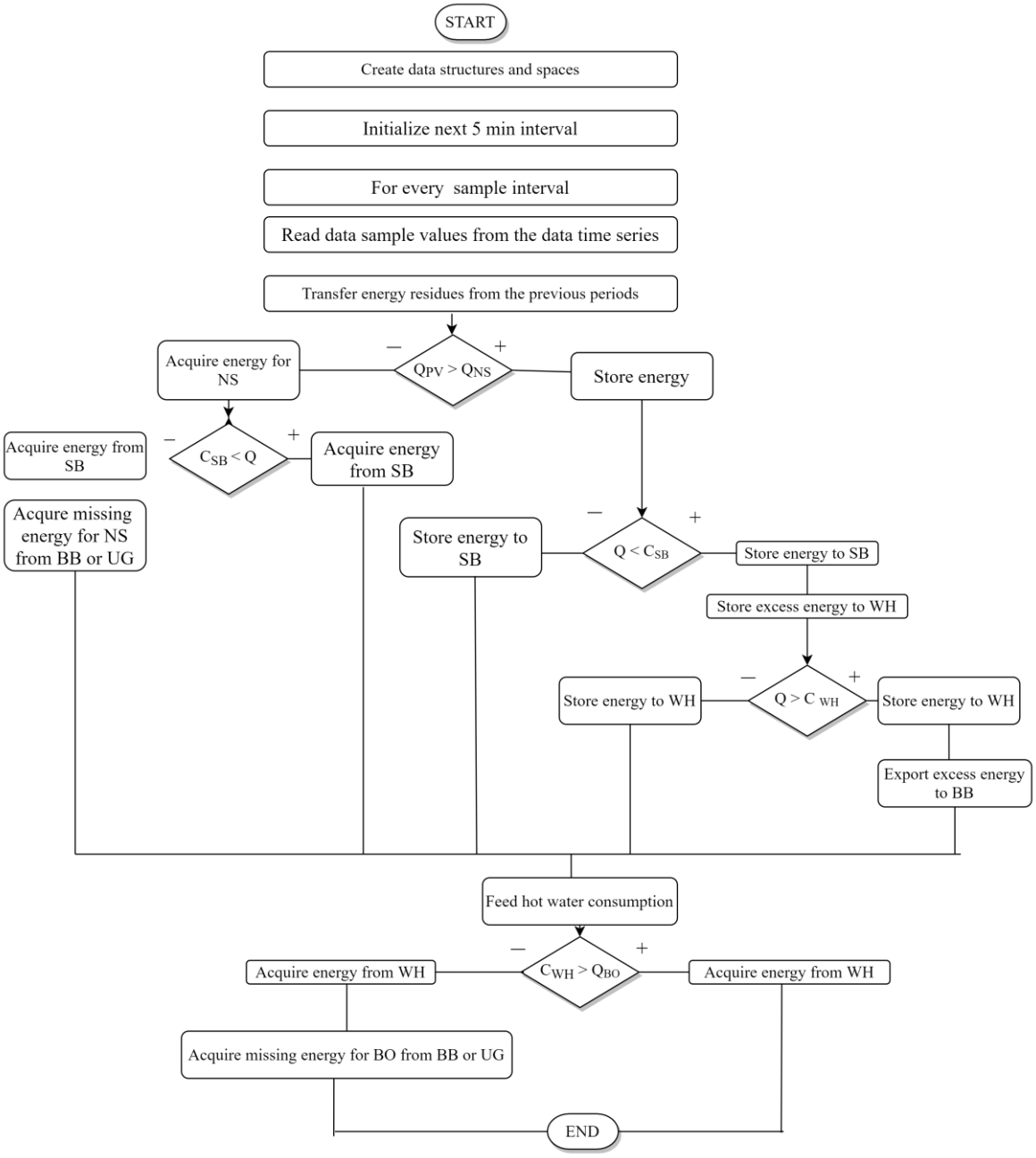

Figure 3. Flowchart of the developed nanogrid algorithm.

In Figure 3 (all symbols are featured in energy units, kWh):

Q is variable, depending on current situations;

Q_{PV} is the 5-min energy production from PV (in Figure 1, Arrow E;

Q_{NS} is the 5-min energy consumption of graph NS (in Figure 1, Arrow H);

Q_{WH} is the 5-min energy feed-in WH (in Figure 1, Arrow I);

Q_{BO} is the 5-min energy consumption of the BO graph (in Figure 1 Arrow J);

C_{WH} is the current energy content in WH, but not more than C_{WHmax} as set maximum capacity in particular calculation step;

C_{SB} is the current energy content in SB, but not more than C_{SBmax} as set maximum capacity in particular calculation step;

C_{BB} is the current energy content of BB, but not more than C_{BBmax}, which sets maximum capacity in specific calculation steps. As a reminder, SB means nanogrid battery, and BB is buffer battery.

When the energy from the PV in the 5-min run has been compared to the NS requirements, the controller will decide on the NS's energy needs a source.

If the PV does not receive enough energy for NS, the missing energy is taken from SB.

If inequality $Q_{PV} > Q_{NS}$ is true, then the surplus energy to meet NS needs will move to SB if SB is full to WH.

Suppose WH is full; then energy moves to BB. In case of lack of additional space for energy in BB, then to UG.

If inequality $Q_{PV} > Q_{NS}$ is not valid, it will be taken short of energy from SB; if it is not enough, it will be taken energy from BB or, in case of a lack of energy in BB, Figure 3 has been simplified for better insight. After filling the WH from the PV through the NS, the scheduled energy BO consumption is taken from the WH. If there is more space in the WH, additional PV energy will be added through the NS. This part of the program is not shown in Figure 3.

The block "Export excess energy to BB" is denoted in Figure 1 as Arrow C.

The peaks of the PV generation schedules correspond to the relatively small amount of energy, which could allow for a noticeably reduced power rating of the inverter without a significant impact on the cover factor. This could enable certain cost savings.

The decision-making blocks formally concern a single sequence process, which starts with the assessment that the energy produced by the PV at the ith of the 5-minute interval can be fully supplied to the NS consumer. The following order of transmission and allocation of energy is as follows: WH, BB and UG. If not PV produces enough energy for NS consumption, it is taken from SB or followed by BB or UG. If the energy generated by PV is leftover from NS consumption, then priority will be given to adding the surplus to SB first. Such a sequential process [39] is technically possible, where the Smart Meter distributes energy flows as follows: first, to UG, the remaining energy to the NS (here is also included in NS with BO), and finally, using a particular additional module, all the remaining energy, as far as it is received, goes to BO.

2. Results and Discussion

A simulation has been carried out to achieve the objectives of this work. The energy system of a private house (Figure 1) is included in the simulation model with load and unloading characteristics. Model input variables are yearlong time series PV production, consumption NS and BO patterns.

To assess the coincidence of the production schedule and load graph, the cover factor in Equation 1 is applied. The simulation carried out is based on the flow chart in Figure 3.

Based on earlier research [33, 36], the values of such nanogrid equipment parameters for numerical simulation experiments have been fixed, SB = 3 kWh and WH = 5 kWh. The amplification coefficient RS has been used to find dependence on PV panel energy production to nanogrid through BB to UG, Arrow D and conversely Arrow A in Figure 1. The RS rate is the ratio of PV energy supplied to NG to the energy consumed in nanogrid during the same period. Figure 4 shows the energy flows in RS ranges from 0.8 to 3. At the intersection of two lines, R_S = 1, absorbed and injected energies are equal. The energy taken from the UG shows a slightly linear falling line. In Figure 4, equilibrium in R_S = 1, the amounts of energy taken from and given from UG equal 1374 kWh. Even a small over-dimensioning of PV compared to annual consumption will significantly increase the direction of energy exchange to UG [40-43]. R_S in further increase indicates a linearly growing amount of electricity given to straight UG.

In Figure 5, we have set BB's maximum value up to 50 kWh. From Figure 5, we can see that the operations have already stabilised at BB = 30 kWh. Next, consider the processes up to BB = 30 kWh.

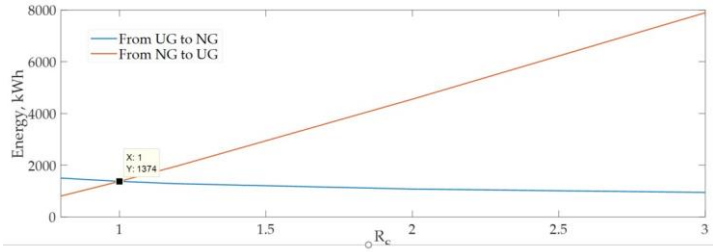

Figure 4. Dependence of energy flows on different *Rs* rates without BB on an annual basis.

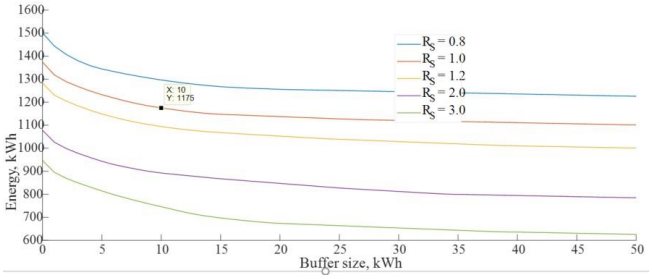

Figure 5. Energy from the utility grid (UG) to nanogrid (NG).

The following analysis examines the energy flow dependencies according to BB size. By setting BB to a twist of 10 kWh, Figure 5 has a UG-to-NG energy flow equal to 1175 kWh, while the resulting energy flow BB-to-NG is shown in Figure 6 is 198,9 kWh. The sum of these two values is 1374 kWh, equal to the situation without BB in Figure 4. The analogous approach is also applicable to other BB and *Rs* sizes.

Figure 7 shows that the most significant Y_D increments are only released BB = 10 kWh, above which there is already stabilisation. Increasing PV annual output to double will give us a Y_D growth of 0.081. This growth represents 12.2 % of the original Y_D value at R_S = 1.

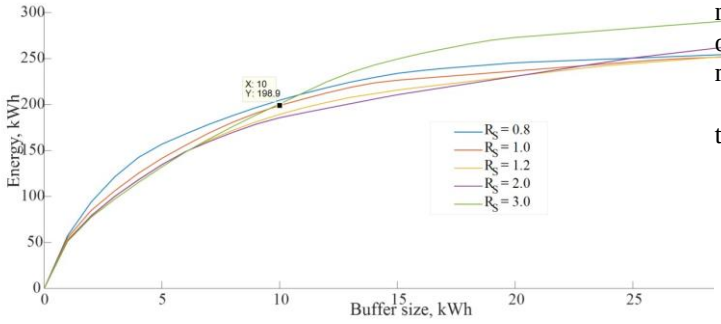

Figure 6. Energy exchange from buffer battery (BB) to nanogrid (NG) and amplification coefficient (RS) size.

Figure 6 shows the energy flows from BB to NG (Figure 1 (B)). The amounts of energy shown on the y-axis are the fourth member W4 on the fraction line of Formula 1.

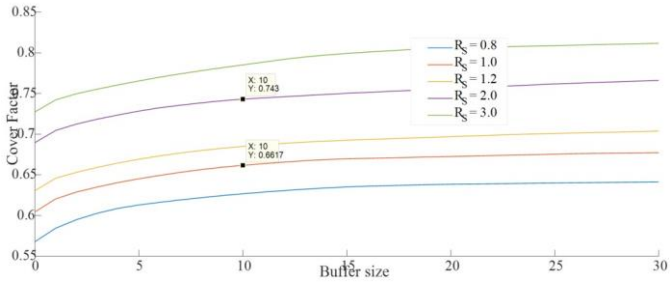

Figure 7. Dependencies to demand cover factor from buffer battery volume (BB) and amplification coefficient (R_S) size.

Table 1. Comparison of PV and wind-powered nanogrid solutions.

Parameter	Wind [31]	PV
P_{nom} (kW)	5	3.67
WH (kWh)	6	5
SB (kWh)	6	3
R_S = 1, without BB (kWh)	1401	1374
From UG to NG with BB = 10 kWh	1180	1175
From BB to NG with BB = 10 kWh	221	198.9
Y_D BB = 0 R_S = 1	0.597	0.604
Y_D BB = 10 R_S = 1	0.660	0.662
Y_D BB = 0 R_S = 2	0.724	0.689
Y_D BB = 10 R_S = 2	0.796	0.744

Table 1 shows that the NG with BB works similarly for wind and PV panel power. However, the need for storage devices when using PV energy is much lower. The need for the battery is even halved. If the price of WH does not depend so much on its capacity, then it is already noticeable in the case of batteries. If the annual production of a wind generator is doubled, its effect on Y_D will be more significant than using PV.

Figure 8 shows the inverter capacity's influence on the demand cover factor rates.

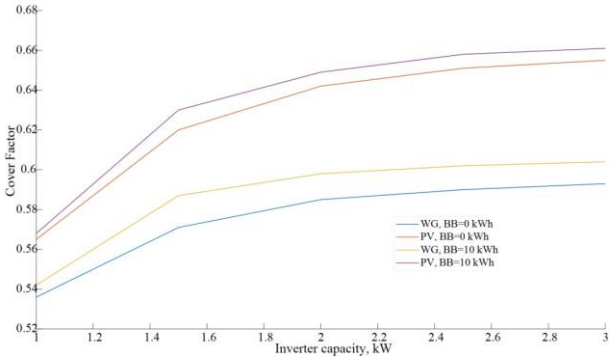

Figure 8. Dependence of demand cover factor from the inverter-rated power.

Based on Table 1 data, the P_{nom} of WG = 5 kW and PV = 3.67 kW. In both cases, we set the initial power of the inverter to 3 kW. Figure 8 shows WG values at the lower level and PV values at a higher level, as expected. It also indicates that the sharper decline in demand cover factor begins at the limited power of the inverter at 1.5 kW.

3. Conclusion

This article analysed the NG of a private house with PV generation connected to UG through BB.

The main results of this work are as follows:

- The PV panel-powered solution (WH = 5 kWh, battery = 3 kWh) compared to the wind power (both are 6 kWh) requires smaller storage devices to achieve the same cover factor.
- Append in PV-powered NG system 10 kWh BB capacity between NG and UG, by R_S = 1, when rising Y_D = 0.604…0,662. This means the increment is Δ Y_D = 0.058 or 9.6 % in relative units.
- By rising in PV powered system R_S = 1 to R_S = 2, by BB = 10 kWh when rising Y_D = 0.662…0.743. This means the increment is Δ Y_D = 0.081 or 12.2 % in relative units.
- If we use both methods simultaneously, increase the R_S mentioned in the previous paragraphs, and together BB= 10 kWh, we get the whole Y_D for the resultant increase Y_D = 0.604 to 0.743. This means the increment is Δ Y_D = 0.139 or 23 % in relative units. Economically, it makes more sense to increase Y_D than to increase BB, but BB amplifies the Y_D effect.
- Reducing the inverter's rated power by up to 50% does not significantly reduce the demand cover factor.

Acknowledgements

The authors would like to thank the Estonian Centre of Excellence in Zero Energy, and Resource Efficient Smart Buildings and Districts, ZEBE, grant TK146 funded by the European Regional Development Fund supported this research, and Alo Allik for measuring consumption data for this study.

References

[1] Energy Efficiency Directive. Available online: https://ec.europa.eu/energy/topics/energy-efficiency/targets-directive-and-rules/energy-efficiency-directive_en strategy (accessed on 10 July 2021).

[2] N. Naval, R. Sánchez, and J.M. Yusta, "A virtual power plant optimal dispatch model with large and small-scale distributed renewable generation", Renewable Energy 2020, 151, 57-69. https://doi.org/10.1016/j.renene.2019.10.144

[3] S. Bounouar, R. Bendaoud, H. Amiry, B. Zohal, F. Chanaa, E. Baghaz, C. Hajjaj, S. Yadir, A. El Rhassouli, and M. Benhmida, "Assessment of Series Resistance Components of a Solar PV Module Depending on its Temperature Under Real Operating Conditions," International Journal of Renewable Energy Research (IJRER), no. 4, December, pp. 1554-1565, 2020.

[4] J. Lepa, A. Annuk, E. Kokin, V. Põder, and K. Jürjenson, "Energy Production and Consumption Charts in Energy System," Oil Shale, vol. 26, no. 3, pp. 309-318, 2009. doi:10.3176/oil.2009.3S.12

[5] J. Lepa, E. Kokin, A. Annuk, V. Põder, and K. Jürjenson, "Wind Power Stations Performance Analysis and Power Output Prognosis," in Engineering for Rural Development, Jelgava, pp. 92-96, 28-29 May 2008.

[6] B.R. Ravada, N.R. Tummuru, and B.N.L Ande, "Photovoltaic-Wind and Hybrid Energy Storage Integrated Multisource Converter Configuration-Based Grid-Interactive Microgrid", IEEE Transactions on Industrial Electronics, vol.68, pp. 4004-4013, 2021. doi: 10.1109/TIE.2020.2984437

[7] S. Kotra, and M.K. Mishra, "A Supervisory Power Management System for a Hybrid Microgrid With HESS," IEEE Transactions on Industrial Electronics, vol. 64, no. 5, May 2017, pp. 3640-3649. doi: 10.1109/TIE.2017.2652345

[8] I.B. Bakken, and M. Korpås, "Energy Storage Scheduling in Distribution Systems Considering Wind and Photovoltaic Generation Uncertainties," Energies, vol. 12, 1231, 2019. https://doi.org/10.3390/en12071231

[9] K. Kusakana, "Optimal peer-to-peer energy management between grid-connected prosumers with battery storage and photovoltaic systems," Journal of Energy Storage, vol. 32, 101717, 2020. https://doi.org/10.1016/j.est.2020.101717

[10] K. Jana, A. Ray, M.M. Majoumerd, M. Assadi, and S. De, "Polygeneration as a future sustainable energy solution," Applied Energy, vol. 202, pp. 88-111, 2017. https://doi.org/10.1016/j.apenergy.2017.05.129

[11] G. Y. Abusaibaa, A. B. Alaasam, A. H. A. Alwaeli, and A. W. A. Alfatlawi, "Performance Analysis of Solar Absorption Cooling Systems in Iraq," International Journal of Renewable Energy Research (IJRER), vol. 10 no. 1, pp. 224-230, 2020.

[12] A. Al-Kassem, M. A. Ahmadi, and A. Draou, "Modeling and Simulation Analysis of a Hybrid PV–Wind Renewable Energy Sources for a Micro-grid Application," In Proceedings of 9th International Smart Grid Conference, 28 June-1 July 2021, Setubal, Portugal. pp. 103-106, 2021. DOI: 10.1109/icSmartGrid52357.2021.9551215

[13] Y. Sun, S. Wang, F. Xiao and D. Gao, "Peak load shifting control using different cold thermal energy storage facilities in commercial buildings: A review," Energy Conversion and Management, vol. 71, pp. 101-114, 2013. https://doi.org/10.1016/j.enconman.2013.03.026

[14] S. Duerr, C. Ababei, and D. M. Ionel, "Load balancing with energy storage systems based on co-simulation of multiple smart buildings and distribution networks," In Proceedings of 6th Int. Conf. Renew. Energy Res. Appl., 5-8 December 2017, San Diego, USA, pp. 175-180, 2017. doi:10.1109/ICRERA.2017.8191262

[15] A. Allik, and A. Annuk, "Transient Process in Small Scale Autonomous Photovoltaic and Wind Power Systems," In Proceedings of 6th Int. Conf. Renew. Energy Res. Appl., vol. 6, pp. 159-163, 2017. 5-8 December 2017, San Diego. doi:10.1109/ICRERA.2017.8191259

[16] R. Baetens, J. De Coninck, J. Y. Roy, B. Verbuggen, J. Driese, L. Helsen, and D. Saelens, "Assessing electrical bottlenecks at feeder level for residential net zero energy buildings by integrated system simulation," Applied Energy, vol. 96, pp. 74-83, 2012. https://doi.org/10.1016/j.apenergy.2011.12.098

[17] A.A. Bashir, M.P. Kasmaei, A. Safdarian, and M. Lehtonen, "Matching of Local Load with On-Site PV Production in a Grid-Connected Residential

Building," Energies 2018, 11, 2409. https://doi.org/10.3390/en11092409

[18] M.Z. Degefa, M. Lehtonen, M. McCulloch, and K. Nixon, "Real-time matching of local generation and demand: The use of high-resolution load modelling," IEEE PES Innovative Smart Grid Technologies Conference Europe. Book Series: IEEE PES Innovative Smart Grid Technologies Conference Europe. 2016. doi:10.1109/ISGTEurope.2016.7856186

[19] J. Drücke, M. Borsche, P. James, F. Kaspar, U. Pfeifroth, B. Ahrens, and J. Trentmann, " Climatological analysis of solar and wind energy in Germany using the Grosswetterlagen classification," Renewable Energy, vol. 164, pp. 1254-1266, 2021. https://doi.org/10.1016/j.renene.2020.10.102

[20] A. Annuk, A. Allik, P. Pikk, J. Uiga, H. Tammoja, K. Toom, and J. Olt, "Increasing renewable fraction by smoothing consumer power charts in grid-connected wind-solar hybrid systems," Oil Shale, vol. 30, no. 2S, pp. 257-267, 2013. doi: 10.3176/oil.2013.2S.06

[21] A. Annuk, W. Yaïci, A. Blinov, M. Märss, S. Trashchenkov, and P. Miidla, "Modelling of Consumption Shares for Small Wind Energy Prosumers," Symmetry 2021, 13, 647. https://doi.org/10.3390/sym13040647

[22] F. Sharma, H. Radjeai, S. Mouss, and A. Chouder, "New algorithm for energy dispatch scheduling of grid-connected solar photovoltaic system with battery storage system," Electrical Engineering&electromechanics, vol. 1, pp. 27-34, 2021. doi: 10.20998/2074-272X.2021.1.05

[23] P. Mirhoseini, and N. Ghaffarzadech, "Economic battery sizing and power dispatch in a grid-connected charging station using convex method," Journal of Energy Storage, vol. 31, 101651, 2020.

https://doi.org/10.1016/j.est.2020.101651

[24] W. Praiselin, and J.B. Edward, "Improvement of Power Quality with Integration of Solar PV and Battery Storage System Based Micro Grid Operation," International Conference on Innovations in Power and Advanced Computing Technologies [i-PACT2017], pp.1-5, 2017 doi: 10.1109/ipact.2017.8245082

[25] A.I. Nusaif, and A.L. Mahmood, "MPPT Algorithms (PSO, FA, and MFA) for PV System Under Partial Shading Condition, Case Study: BTS in Algazalia, Baghdad," International Journal of Smart Grid, vol. 10, pp. 100-110, 2020.

[26] A. Belkaid, I. Colak, K. Kayisli, and R. Bayindir, "Design and Implementation of a Cuk ConverterControlled by a Direct Duty Cycle INC-MPPT in PV Battery System," International Journal of Smart Grid, vol. 3, pp. 19-25, 2019.

[27] A.H. Sabry, A.H. Shallal , H.S. Hameed, and P.J. Ker, "Compatibility of household appliances with DC microgrid for PV system," Heliyon, vol. 6, 2020, e05699. https://doi.org/10.1016/j.heliyon.2020.e05699

[28] A. Barzkar, and S.M.H. Hosseini, "A novel peak load shaving algorithm via real-time battery scheduling for residential distributed energy storage systems," International Journal of Energy Research, vol. 42, pp. 2400-2416, 2018. https://doi.org/10.1002/er.4010

[29] E. Reihani, M. Motalleb, R. Ghorbani, and L.S. Saoud, "Load peak shaving and power smoothing of a distribution grid with high renewable energy penetration," Renewable Energy, vol. 86, pp. 1372-1379, 2016. https://doi.org/10.1016/j.renene.2015.09.050

[30] B. Kroposki, T. Basso, and R. DeBlasio, "Microgrid standards and technologies," in the IEEE Power and Energy Society 2008 General Meeting: Conversion and Delivery of Electrical Energy in the 21st Century, PES, Pittsburg, PA, USA, 20-24 July 2008; doi:10.1109/PES.2008.4596703

[31] A. Annuk, W. Yaïci, M. Lehtonen, R. Ilves, T. Kabanen, and P. Miidla, "Simulation of Energy Exchange between Single Prosumer Residential Building and Utility Grid," Energies, vol. 14, 1553, 2021. https://doi.org/10.3390/en14061553

[32] H. F. Naspolini, and R. Rüther, "The effect of measurement time resolution on the peak time power demand reduction potential of domestic solar hot water systems," Renewable Energy, vol. 88, pp. 325-332, 2016.

[33] S.I. Sun, B.D. Smith, R.G.A. Wills, and A.F. Crossland, "Effects of time resolution on finances and self-consumption when modelling domestic PV-battery systems," Energy Reports, vol. 6, pp. 157-160, 2020. https://doi.org/10.1016/j.egyr.2020.03.020

[34] A. Burgio, D. Menuti, N. Sorrentino, A. Pinnarelli, and Z. Leonovicz, "Influence and Impact of Data Averaging and Temporal Resolution on the Assessment of Energetic, Economic and Technical Issues of Hybrid Photovoltaic-Battery Systems," Energies, vol. 13, 354, 2020. https://doi.org/10.3390/en13020354

[35] A. Annuk, M. Hovi, J. Kalder, and M. Märss, "Consumption and wind production time series data," Estonian University of Life Sciences, Tartu, 2020. https://doi.org/10.15159/eds.dt.20.02 (accessed on 10 July 2021).

[36] A. Annuk, M. Hovi, J. Kalder, T. Kabanen, R. Ilves, M. Märss, B. Martinkauppi, and P. Miidla, "Methods for increasing shares of self-consumption in small PV solar energy applications," In Proceedings of 9th International Conference on Renewable Energy Research and Applications (ICRERA) 2020), Glasgow, UK, 26-29 September 2020, Vol. 5, pp. 184-188. doi: 10.1109/ICRERA49962.2020.9242902

[37] D. Vanhoudt, D. Geysen, B. Claessens, F. Leemans, L. Jespers, and J. Van Bael, "An actively controlled residential heat pump: Potential on peak shaving and maximization of self-consumption of renewable energy," Renewable Energy, vol. 63, pp. 531-543, 2014. https://doi.org/10.1016/j.renene.2013.10.021

[38] I.B. Sperstad, and M. Korpås, "Energy storage scheduling in distribution systems considering wind and photovoltaic generation uncertainties," Energies, vol. 12, 1231, 2019. doi:10.3390/en12071231

[39] Fronius Smart Meter. https://www.mcelectrical.com.au/the-fronius-smart-meter/#:~:text=%20The%20Real%20Solution%20%201%20The%20Datamanager.,from%20the%20Data manager%20and%20the%20smart...%20More%20 (accessed on the 10 July 2021)

[40] J.M. Lujana-Rojas, R. Dufo-Lopez, J.L. Bernal-Agustin, I.A. Domínguez-Navarro, and J.P.S. Catalao. "Probabilistic perspective of the optimal distributed generation integration on a distribution system," Electrical Power Systems Research, vol. 176, pp. 9-20, 2019. https://doi.org/10.1016/j.epsr.2018.10.015

[41] S. Boulmrharj, R. Rabeh, V. Felix, R. Ouladsiner, M. Bakhouya, K. Zine-Dine, M. Khaidar, and M. Siniti, "Modeling and Dimensioning of Grid-Connected Photovoltaic Systems," in 2017 International Renewable and Sustainable Energy Conference (IRSEC), Tangier, Morocco, pp. 1-6, 4-7 December 2017. DOI: 10.1109/IRSEC.2017.8477392

[42] H. Zhang, J. Cai, K. Fang, F. Zhao, and J.W. Sutherland, "Operational optimization of a grid-connected factory with onsite photovoltaic and battery storage systems," Applied Energy, vol. 205, pp. 1538-1547. 2017. https://doi.org/10.1016/j.apenergy.2017.08.140

[43] J. Hirvonen, G. Kayo, S. Cao, A. Hasan, and S. K. Siren, "Renewable energy production support schemes for residential-scale solar photovoltaic systems in Nordic conditions," Energy Policy, vol. 79, pp. 72-86, 2015. https://doi.org/10.1016/j.enpol.2015.01.014